

10536 2614 NI ACAN
NACA TN 4197 95501

TECH LIBRARY KAFB, NM
0066822

TECHNICAL NOTE 4197

NATIONAL ADVISORY COMMITTEE
FOR AERONAUTICS
SUMMARY OF FLUTTER EXPERIENCES AS A GUIDE TO
THE PRELIMINARY DESIGN OF LIFTING

SURFACES ON MISSILES

TECHNICAL NOTE 4197
By Dennis J. Martin

Langley Aeronautical Laboratory
Langley Field, Va.

SUMMARY OF FLUTTER EXPERIENCES AS A GUIDE TO
THE PRELIMINARY DESIGN OF LIFTING

SURFACES ON MISSILES

By Dennis J. Martin

Langley Aeronautical Laboratory
Langley Field, Va.

Washington
February 1958



Washington
February 1958

ASMEC
TECHNICAL LIBRARY
7-1-2011



0066822

NATIONAL ADVISORY COMMITTEE FOR AERONAUTICS

TECHNICAL NOTE 4197

SUMMARY OF FLUTTER EXPERIENCES AS A GUIDE TO
THE PRELIMINARY DESIGN OF LIFTING
SURFACES ON MISSILES¹

By Dennis J. Martin

SUMMARY

A limited review is made of some experiences in the flight testing of missiles and of wing flutter investigations that may be of interest in missile design. Several types of flutter which may be of concern in missile studies are briefly described. Crude criteria are presented for two of the most common types of flutter to permit a rapid estimate to be made of the probability of the occurrence of flutter. Many of the details of the flutter picture have been omitted, and only the broader elements have been retained so as to give the designer an overall view of the subject.

INTRODUCTION

Many different types of flutter may be encountered on airplanes, propellers, helicopters, and missiles and the speed ranges and conditions encountered lead to flutter phenomena that are widely different. Broadly speaking, the phenomenon of flutter is generally concerned with vibrations or oscillations of a lifting surface. Oscillations of a lifting surface give rise to oscillations of the aerodynamic forces which in turn, under certain conditions, may have phase characteristics that increase the oscillations to dangerous amplitudes. Some types of flutter may be mild; others may be disastrous. Flutter may involve fully established flow or broken-down flow, high or low frequencies of the structure, and one or more modes of vibration.

The missile not only experiences many of the flutter problems encountered with airplanes but also presents many new and different problems, depending upon the design and purpose of the missile. Examples are: skin flutter, flutter of automatic controls or servomechanisms,

¹Supersedes declassified NACA Research Memorandum L51J30 by Dennis J. Martin, 1951.

and flutter of short wings with ram jets or external stores. Many of these types of flutter can best be studied by difficult experiments; others require long and tedious theoretical investigations. For the more common types there exist sufficient experimental data to evaluate simple criteria. In general so many factors enter into a flutter case that a comprehensive criterion becomes quite unwieldy. Simple criteria must neglect or restrict many parameters. Furthermore, there are possibilities for exception; hence any simple criterion should not be considered as perfectly general. In spite of these limitations a criterion does have some usefulness in estimating the probability of a particular type of flutter occurring for a given configuration.

In this paper two simple criteria are presented. The first is for the most common type, the wing bending-torsion flutter. Another is presented for stall flutter, and a brief discussion is included of pitch-bending flutter.

SYMBOLS

A	panel aspect ratio
a	velocity of sound; also, nondimensional distance of elastic axis behind the midchord expressed as a fraction of the semichord
b	semichord
c	chord
$f_1(\lambda)$	approximate function relating torsional frequency of a tapered panel to that of an untapered panel
$f_2(\lambda)$	function relating the chord of a tapered panel at the panel three-quarter span to the chord at the panel midspan
G_E	effective shear modulus of an equivalent section
I	moment of inertia about elastic axis
J	section torsional modulus
J_S	section torsional modulus of a solid section
JG	torsional stiffness parameter

L	panel span
M	Mach number
m	mass per unit span
N	calculated parameter (two-dimensional incompressible flutter speed divided by velocity of sound)
n	empirical number used in aspect-ratio correction
p	fluid pressure
r_{α}	nondimensional radius of gyration relative to elastic axis, expressed as fraction of semichord
t	section thickness
V	velocity
V_f	flutter velocity
X	nondimensional geometric parameter, defined in appendix
x	distance of wing leading edge behind the missile center of gravity
x_{α}	nondimensional distance of section center of gravity behind elastic axis expressed as fraction of semichord
α	angle of attack measured from zero lift
Λ	sweep angle of wing midchord line
λ	taper ratio (ratio of tip chord to root chord)
ϵ	nondimensional distance of section center of gravity behind wing quarter-chord expressed as fraction of chord
κ	relative density parameter
ρ	fluid density
ω_{α}	angular wing torsional frequency
ω_h	angular wing bending frequency

Subscripts:

0.50 panel midspan station

- 0.75 panel three-quarter-span station
- 0 sea-level standard conditions

DISCUSSION OF CRITERION

Types of Flutter

Examples of some of the more common modes that may interact during flutter are given in figure 1. The first example shown is the most common type of flutter encountered; in this type of flutter the elastic modes of the wing (wing bending and wing twisting or torsion) combine to extract energy from the air stream, that is, to produce flutter. In addition, a control surface may interact significantly with these motions to produce other types of flutter. The second example shown in figure 1 illustrates a type of flutter which involves only one motion or degree of freedom. The type of flutter illustrated occurs at high angles of attack and is commonly known as stall flutter. Only a torsional twisting motion of the wing is present. There are other motions that may produce a single-degree flutter of the type illustrated by this stall-flutter case. Examples are: aileron buzz, single-degree bending oscillations of swept wings, and single-degree pitching oscillations of a wing. The third example in figure 1 illustrates a type of flutter in which the motion of the whole fuselage enters significantly into the flutter. This example illustrates a pitching motion of the entire missile combined with a bending motion of the wing. Other body motions (rolling, yawing, vertical translation, and so forth) also may enter into flutter.

Bending-Torsion Flutter

In order to illustrate the significance of the first criterion to be presented for the most common flutter, wing bending-torsion flutter, figure 2 (see references 1 and 2) has been prepared to show the flutter behavior of wings over a range of Mach numbers. Shown in this figure is the actual flutter Mach number plotted against a calculated quantity N , which is dependent upon the wing stiffness, center-of-gravity location, mass ratio, certain aerodynamic quantities, and so forth. The parameter N is an orderly combination of many of the parameters that are important in flutter. The flutter expert may recognize this N as the calculated two-dimensional incompressible flutter speed divided by the velocity of sound. Typical curves for wings of zero sweep and full-span aspect ratios of 2 and 7 are shown, and an approximate curve is shown for a wing of 60° sweepback and aspect ratio 4. As the value of N for the aspect-ratio-7 wings is increased, for example, by

increasing the wing torsional stiffness or by increasing the operating altitude, the flutter Mach number is seen to increase and a value of N is eventually reached which will not produce an intersection with the flutter boundary. The significance of this result is that, if the wing is so stiff or if the quantity N is so large that flutter is not encountered in this region around a Mach number of 1 (for the higher aspect ratios), flutter of the type considered herein would not be expected to occur at higher Mach numbers. It is this maximum or critical value of the quantity N that is of interest in missile design, because missiles must operate throughout the Mach number range. It must be emphasized that the curves for other aspect ratios, sweep angles, and so forth may appear quite different from the one shown for the aspect-ratio-7 wings and hence may have a different critical Mach number range and a different value of N required for the wing to be flutter-free. If all the critical values of this parameter N that are necessary to avoid flutter were known for the various aspect ratios, sweep angles, thickness ratios, section properties, and so forth, the flutter problem for missile design would be greatly simplified.

Investigations in the Langley 9- by 18-inch supersonic flutter tunnel have attempted to define values of N for various supersonic Mach numbers. (See refs. 3, 4, and 5.) Many of these data, together with many data from the Langley Pilotless Aircraft Research Division on missiles and bombs which experienced no known flutter difficulties, as well as on missiles on which flutter was attained, have been accumulated. This store of experience has been compared to a simplified and modified criterion which groups the significant parameters in a manner similar to that used for N in an attempt to establish limits of the critical values of the structural and aerodynamic requirements for a wing to be flutter-free. This criterion is based on modifications to an approximate flutter formula proposed by Theodorsen and Garrick (ref. 6). This formula was for high-aspect-ratio, heavy wings having a low ratio of bending to torsional frequency. The application of modifications of this formula to include low-aspect-ratio wings including swept and highly tapered wings is admittedly stretching the basic formula; nevertheless, in the present study this approach has been made, and the parameters have been adjusted until a reasonable coherence in the results was obtained. For simplicity this modified criterion is broken down into simple geometric dimensions and structural properties. (This modification is described in the appendix.) The experimental data which have been accumulated are then compared, and an attempt is made to bracket the safe wings and the unsafe wings. This comparison is made in figure 3.

Plotted against the effective shear modulus of the wing material is the ratio of the fluid pressure to standard pressure p/p_0 times $\frac{\lambda + 1}{2}$, where λ is the taper ratio, times a quantity X which is

obtained from the geometric dimensions of one wing panel. (See appendix.) The abscissa G_E is the effective shear modulus of the wing structure and is indicated for wings of solid wood, magnesium, aluminum, titanium, and steel. A solid wing of, say, aluminum would fall at the point marked along the abscissa while a fabricated wing of aluminum would have a lower effective G_E and would fall somewhat to the left, depending upon the skin thickness and spar size. The value of G_E can be determined for fabricated wings from a measured value of the torsional stiffness parameter JG by the relation $G_E = \frac{6(JG)_{\text{measured}}}{ct^3}$, where c is the chord and t is the thickness. The quantity X noted in the ordinate is shown in figure 4 as a function of the panel aspect ratio for constant values of the thickness ratio in the streamwise direction. It must be remembered that the abscissa of this figure is the exposed aspect ratio of only one wing panel as distinguished from the normal aspect ratio which includes both wings and the fuselage.

Shown in figure 3 are data taken from subsonic, transonic, and supersonic wind tunnels and from rocket and bomb-drop tests for both swept and unswept wings. The open points are for missile wings that traversed the Mach number range to at least a Mach number of 1.3 or higher without known failure. The solid points are for missile and wind-tunnel tests where flutter or failure occurred. It must be pointed out that some of the data are for missiles that were designed primarily for aerodynamic research. The instrumentation of these missiles was, therefore, not usually of a type that could definitely indicate that no oscillations occurred for the cases represented by open points or that the failures for the cases represented by the solid points were due to flutter rather than some other cause. The many data shown tend to indicate that two regions can be defined in which the open and solid points are reasonably well separated and the flutter region is established. The shaded area indicates a probable division based on the existing data. This chart is useful in estimating the probability of the occurrence of flutter of the bending-torsion type for a given configuration. A designer may see where a given design lies with respect to many other designs which did or did not experience flutter problems.

As an illustration, if a design had an exposed-wing-panel aspect ratio of 2 and a streamwise thickness ratio of 4 percent, from figure 4 a value of X of about 1.25×10^6 pounds per square inch is indicated. If the missile were ground-launched, that is, at standard pressure $\frac{p}{p_0} = 1$, and if the wing were untapered, that is $\frac{\lambda + 1}{2} = 1$, then the ordinate of figure 3 for this design would be 1.25×10^6 ; and if the construction were solid magnesium, it would plot in the flutter

region and would most probably be unsafe. If the wing were of solid aluminum, it would be marginal. Further detailed analysis or experiment would be needed to complete this design. However, if the wing were of solid steel, it would probably be safe, at least insofar as the bending-torsion type of flutter considered is concerned.

As another example, suppose the material of construction has already been selected, titanium for instance. In order to allow a reasonable margin of safety an ordinate of figure 3 of about 0.8 or less might be specified. If the wing were untapered and ground-launched, the ordinate of figure 4 is then 0.8 and it can be seen that for a panel aspect ratio of 1 a thickness ratio of 2.5 percent is required. For an aspect ratio of 2 a thickness of 4.5 percent is required, and for an aspect ratio of 3 a thickness of about 6.5 percent must be used so that the design may most likely be free of the bending-torsion type of flutter for which this figure applies.

Stall Flutter

There are many other types of flutter that may occur under certain conditions, and they must also be investigated. With a change in the type of flutter, a change must be made in the type of criterion. As mentioned previously the type of flutter that may be encountered depends upon the design and purpose of the missile. As an example of the dependence of the type of flutter upon the use of the missile, it may be mentioned that high-angle-of-attack flutter, that is, stall flutter, would probably be considered as possible only for missiles that are required to maneuver sharply. This conclusion is for ground-launched missiles; however, any air-launched missile that is carried externally may be subject to large angles of attack during airplane maneuvers prior to launching and thus may become subject to stall flutter. During a recent bomb-drop test at Langley, a missile-wing failure occurred while the bomb was attached to the airplane. The failure occurred at speeds considerably below the flutter speed subsequently obtained with an identical wing that was protected from the airstream while attached beneath the airplane.

An investigation of stall flutter of thin wings was therefore begun. Although data on stall flutter encountered on missiles are not readily available, a brief discussion of the stall flutter of thin wings and stall flutter of propellers may serve as a rough guide for missile design.

Figure 5 illustrates the flutter behavior of a typical wing at low speeds as the wing produces lift. The ordinate is a nondimensional flutter-speed coefficient $V/b\omega_\alpha$, where V is the flutter speed, b is the half-chord, and ω_α is the torsional frequency. The abscissa is

the angle of attack. As the angle of attack is increased, the flutter speed is reduced drastically. The flutter speed falls rapidly and a minimum is reached at an angle of attack near the stalling angle of the wing.

The flutter encountered at the low angles of attack is of the bending-torsion type which was discussed in the previous figures and was shown to be strongly dependent upon the material of construction. At high angles of attack the flutter occurs essentially in only a torsional mode, and this minimum value of the flutter-speed coefficient $V/b\omega_\alpha$ has been found to be nearly equal to 1 for almost all wings and propeller blades at low speeds, regardless of the material of construction. These results have been confirmed for both wings and propeller blades, and the results are thought to be generally valid for the subcritical-flow speed range. What these curves might look like at supersonic speeds has not been determined; however, a study of the minimum value of $V/b\omega_\alpha$ as affected by Mach number has indicated a beneficial effect at higher speeds. The experimental work of Baker at Langley (reference 7) has suggested that the quantity $b\omega_\alpha$ referred to the speed of sound was a significant parameter for determination of configurations that would be free of stall flutter.

Figure 6 has been prepared to show a comparison of experiment with this parameter $b\omega_\alpha/a$ for a range of Mach numbers. Shown in this figure is the flutter Mach number plotted against $b\omega_\alpha/a$. The curve shown represents the boundary where stall flutter could begin for a given value of $b\omega_\alpha/a$. As $b\omega_\alpha/a$ is increased, for example, by increasing the chord or increasing the torsional frequency, a value is noted to be reached which will not produce an intersection with the flutter boundary. The result is quite similar to the situation that occurred for the bending-torsion flutter (fig. 2).

Baker (ref. 7) has shown that a value of $b\omega_\alpha/a$ of at least 0.5 is required for a propeller to be completely free of stall flutter. Rainey (ref. 8) has substantiated this value of 0.5 for unswept wings of moderate aspect ratio and low structural damping but has indicated, however, that aspect ratio, structural damping, and sweepback may have an influence on the critical value of $b\omega_\alpha/a$. These effects are not well-determined and cannot at present be included in a design chart. The value of $b\omega_\alpha/a$ of 0.5 has nevertheless been used to prepare a design chart for solid unswept wings. Since the torsional frequency times the chord for solid unswept wings is a function only of the length-chord ratio L/c and the thickness ratio and is essentially independent of the material (that is, for such common materials of construction such as steel, aluminum, and magnesium), the design chart (fig. 7) is presented

in terms of the length-chord ratio and the thickness ratio required to attain a value of $b\omega_\alpha/a$ of 0.5. A speed of sound of 1,100 feet per second is assumed.

Wings having geometric quantities which plot above the solid line of figure 7 may experience stall flutter if sufficiently high angles of attack are encountered. It must be remembered that the boundary indicated is for the most critical condition. If the speed range is traversed at low angles of attack, a design may be well above the boundary of this figure without encountering difficulties. This boundary represents only the conditions required for the wing to be completely free of stall flutter throughout the speed range at any angle of attack. The margins of safety for this criterion are not established, and the criterion may have to be modified as more information and data are made available on sweepback, aspect ratio, and structural damping.

Pitch-Bending Flutter

The significance of free-body modes in flutter has been of interest for some time. The problem was considered in early British work on flutter involving the mobility of the fuselage. For example, Broadbent (reference 9) developed simple criteria based on the position of the nodal line. The type of flutter involving missile pitching and wing bending is dependent upon the moment of inertia in pitch of the missile and the bending stiffness of the wing as well as upon the wing location with respect to the center of gravity of the missile. For wings which meet the torsional-stiffness criterion for the bending-torsion type of flutter but are weak in bending, this type of flutter may become important for some wing locations if the missile has a high moment of inertia in pitch. In some flutter tests of rocket vehicles at Langley, several failures have occurred and seemed to involve principally wing bending and missile pitching. The frequency of flutter was somewhat below the first-bending frequency of the wing, near the short-period oscillation of the body. Analyses have been made (ref. 10), and the effect of wing location is illustrated in figure 8.

The ordinate in figure 8 is the flutter-speed coefficient $V/b\omega_h$; in this case the first-bending frequency ω_h is used. The abscissa is the nondimensional distance of the wing behind the center of gravity of the body. The dashed line represents the conventional bending-torsion type of flutter while the solid line shows the effect of inclusion of a body degree of freedom. This flutter speed is much lower than the bending-torsion type for rearward locations and much higher for forward locations. The significant conclusion that can be drawn from these studies of pitch-bending flutter is that the most important consideration is the inclusion of the proper degrees of freedom or modes in the

analysis. Moreover, the observation can be made that, with the change in the type of flutter, a change occurs in the type of flutter criterion; thus in this case the critical speed is affected strongly by the bending stiffness and not by the torsional stiffness as in the case of bending-torsion flutter.

CONCLUDING REMARKS

Simple flutter criteria have been presented to serve as a guide in the preliminary design of lifting surfaces on missiles. The proximity of a configuration to a bending-torsion type of flutter instability may be indicated, and estimates may be made of the probability of the occurrence of flutter by comparison of a given configuration with other designs that have or have not experienced flutter. A simple criterion is presented for stall flutter, and although the margins of safety cannot be established, the criterion may be useful in preliminary design. Pitch-bending flutter is briefly discussed and an example is cited which shows that the wing-bending stiffness and the configuration center-of-gravity position may strongly influence the flutter speed. The discussion of pitch-bending flutter illustrates the case in which a change in the type of flutter can bring about a change in the type of criterion that is needed.

Langley Aeronautical Laboratory,
National Advisory Committee for Aeronautics,
Langley Field, Va., October 16, 1957.

APPENDIX

DERIVATION OF SIMPLIFIED FLUTTER CRITERION

An empirical expression for flutter speed as given by Theodorsen and Garrick (ref. 6) for heavy, high-aspect-ratio wings with a low ratio of bending frequency to torsional frequency is

$$\frac{V_f}{b\omega_\alpha} = \frac{2V_f}{c\omega_\alpha} = \sqrt{\frac{r_\alpha^2}{\kappa} \frac{1/2}{\frac{1}{2} + a + x_\alpha}} \quad (1)$$

If ϵ is substituted for $\frac{\frac{1}{2} + a + x_\alpha}{2}$ (the nondimensional distance of the center of gravity of the section behind the quarter-chord position), equation (1), when squared, becomes

$$V_f^2 = \frac{c^2 \omega_\alpha^2 r_\alpha^2}{16\kappa\epsilon} \quad (2)$$

Experience has generally indicated that more realistic values of V_f are obtained if the quantities in equation (2) are evaluated at the three-quarter spanwise station. Geometrically similar sections are assumed at all spanwise stations; thus, equation (2) becomes

$$\frac{V_f^2}{a^2} = \frac{c_0.75^2 \omega_\alpha^2 r_\alpha^2}{16\kappa\epsilon a^2} \quad (3)$$

where a is the velocity of sound; also

$$r_\alpha^2 = \frac{I}{mb^2} = \frac{4I}{mc^2} \quad (4)$$

and

$$\kappa = \frac{\pi \rho b^2}{m} = \frac{\pi \rho c^2}{4m} \quad (5)$$

The expression for the torsional frequency of a uniform beam is

$$\omega_\alpha = \frac{\pi}{2L} \sqrt{\frac{JG}{I}} \quad (6)$$

Coleman (ref. 11) has given the frequency of a tapered beam of constant thickness ratio in terms of the frequency of an untapered, uniform beam having the same root chord as

$$(\omega_\alpha)_{\text{tapered}} = (\omega_\alpha)_{\text{untapered}} f_1(\lambda) \quad (7)$$

where it has been found that f_1 may be approximated by

$$f_1 \approx 1 + 1.87(1 - \lambda)^{1.6} \quad (8)$$

When equations (4), (5), (6), and (7) are substituted into equation (3), the following is obtained:

$$\frac{V_f^2}{a^2} = \frac{\pi c 0.75^2 f_1^2 JG}{4 \epsilon \rho c^4 L^2 a^2} \quad (9)$$

For a solid, thin airfoil J can be closely approximated by

$$J \approx \frac{ct^3}{6} \quad (10)$$

For a fabricated section, J is extremely difficult to calculate. The value of JG of a section may be experimentally measured and an equivalent solid section may be assumed; thus

$$(JG)_{\text{measured}} = J_S G_E \quad (11)$$

where G_E is an effective shear modulus of the equivalent section; that is,

$$G_E = \frac{6JG}{ct^3} \quad (12)$$

Since $\frac{t}{c}$ is the thickness ratio and $\frac{L}{c_{0.50}}$ is the panel aspect-ratio, equation (9) may be reduced by using equation (12) and the following relations:

$$c_{0.75} = c_{0.50} f_2(\lambda) \quad (13)$$

$$f_2(\lambda) = \frac{1 + 3\lambda}{2(1 + \lambda)} \quad (14)$$

Equation (9) becomes, for wings of constant thickness ratio,

$$\left(\frac{V_f}{a}\right)^2 = \frac{\pi\left(\frac{t}{c}\right)^3 G_E f_1^2 f_2^2}{24\epsilon\rho A^2 b^2} \quad (15)$$

An aspect-ratio correction of the form $\frac{A}{A + n}$ has frequently been used. Reference 12 has suggested a value of $n = 2$. This value of $n = 2$ has been used with success in flutter criteria in reference 13. In the present investigation values of $n = 1, 2, \text{ and } 3$ were tried and the value

of $n = 2$ gave the more consistent results. If the value of $n = 2$ is used, equation (15) becomes

$$\left(\frac{v_f}{a}\right)^2 = \frac{G_E}{\frac{24\epsilon}{\pi} \rho a^2 \frac{A^3}{\left(\frac{t}{c}\right)^3 (A+2)} \frac{1}{f_1^2 f_2^2}} \quad (16)$$

It has been found that $\frac{1}{f_1^2 f_2^2}$ is closely approximated by $\frac{\lambda + 1}{2}$.

By use of the gas law, the following is obtained:

$$\rho a^2 = \gamma p = \gamma p_0 \left(\frac{p}{p_0}\right) \quad (17)$$

The ratio of specific heats $\gamma = 1.4$ is used, and the results apply to air. If a different gas is used, the results must be corrected for a different specific-heat ratio. A value of $\epsilon = 0.25$ is assumed; however, for sections with the center of gravity far from the 50-percent-chord position a correction may be required. Equation (16) becomes

$$\left(\frac{v_f}{a}\right)^2 = \frac{G_E}{\frac{39.3A^3}{\left(\frac{t}{c}\right)^3 (A+2)} \left(\frac{\lambda + 1}{2}\right) \left(\frac{p}{p_0}\right)} \quad (18)$$

Thus, if a critical value of $\left(\frac{v_f}{a}\right)^2$ exists, a plot of the denominator of equation (18) for various materials or values of the numerator, G_E , for missile and wind-tunnel tests may permit a systematic separation to be made of the safe wings and the unsafe wings. The first portion of the denominator of equation (18)

$$X = \frac{39.3A^3}{\left(\frac{t}{c}\right)^3(A + 2)} \quad (19)$$

is calculated and plotted in figure 4.

The value of X can be determined from figure 4 from the thickness ratio and aspect ratio of one exposed wing panel. This value of X is multiplied by $\frac{\lambda + 1}{2}$ and by $\frac{p}{p_0}$ to obtain the ordinate of figure 3.

REFERENCES

1. Lauten, William T., Jr., and Barnby, J. G.: Continuation of Wing Flutter Investigation in the Transonic Range and Presentation of a Limited Summary of Flutter Data. NACA RM L9B25b, 1949.
2. Regier, Arthur A., and Martin, Dennis J.: Recent Experimental Flutter Studies. NACA RM L51F11, 1951.
3. Tuovila, W. J.: Some Experiments on the Flutter of Sweptback Cantilever Wing Models at Mach Number 1.3. NACA RM L51A11, 1951.
4. McCarty, John Locke, and Tuovila, W. J.: Some Flutter Experiments at a Mach Number of 1.3 on Cantilever Wings With Tubular and Closed Bodies at the Tips. NACA RM L53G10b, 1953.
5. Tuovila, W. J., Baker, John E., and Regier, Arthur A.: Initial Experiments on Flutter of Unswept Cantilever Wings at Mach Number 1.3. NACA TN 3312, 1954. (Supersedes NACA RM L8J11.)
6. Theodorsen, Theodore, and Garrick, I. E.: Mechanism of Flutter - A Theoretical and Experimental Investigation of the Flutter Problem. NACA Rep. 685, 1940.
7. Baker, John E.: The Effects of Various Parameters, Including Mach Number, on Propeller-Blade Flutter With Emphasis on Stall Flutter. NACA TN 3357, 1955. (Supersedes NACA RM L50L12b.)
8. Rainey, A. Gerald: Preliminary Study of Some Factors Which Affect the Stall-Flutter Characteristics of Thin Wings. NACA TN 3622, 1956. (Supersedes NACA RM L52D08.)
9. Broadbent, E. G.: Flutter Problems of High Speed Aircraft. Rep. No. Structures 37, British R.A.E., Apr. 1949.
10. Cunningham, H. J., and Lundstrom, R. R.: Description and Analysis of a Rocket-Vehicle Experiment on Flutter Involving Wing Deformation and Body Motions. NACA TN 3311, 1955. (Supersedes NACA RM L50I29.)
11. Coleman, Robert P.: The Frequency of Torsional Vibration of a Tapered Beam. NACA TN 697, 1939.
12. Shornick, Louis H.: The Computation of the Critical Speeds of Aileron Reversal, Wing Torsional Divergence and Wing-Aileron Divergence. MR No. ENG-M-51/VF18, Addendum 1, Materiel Center, Army Air Forces, Dec. 19, 1942.

13. Budiansky, Bernard, Kotanchik, Joseph N., and Chiarito, Patrick T.:
A Torsional Stiffness Criterion for Preventing Flutter of Wings
of Supersonic Missiles. NACA RM L7G02, 1947.

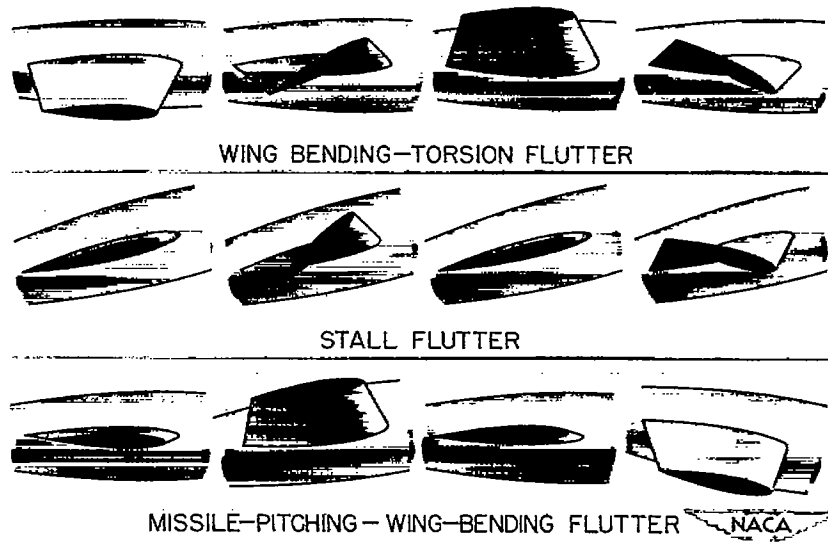


Figure 1.- Examples of flutter modes.

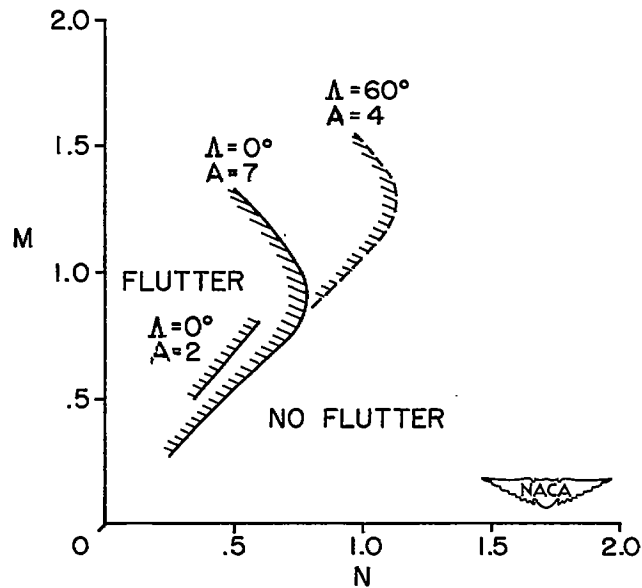


Figure 2.- Trend study of swept and unswept wings at transonic speeds.

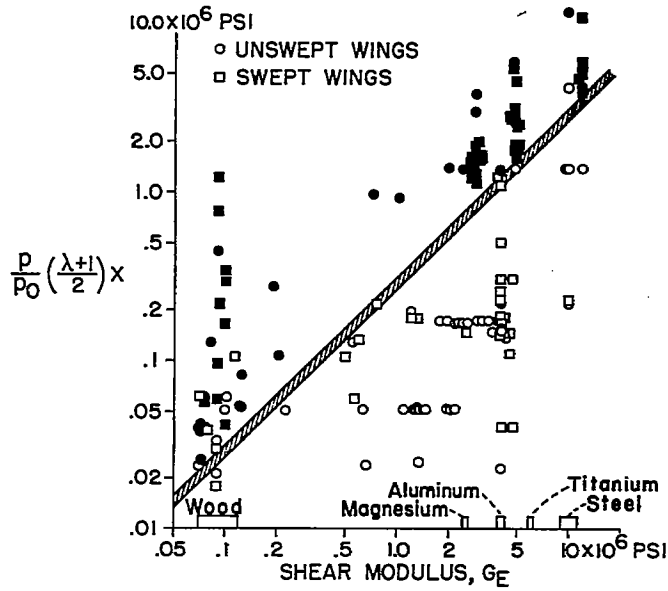


Figure 3.- Composite chart for bending-torsion flutter. $G_E = \frac{6(JG)}{ct^3}$.

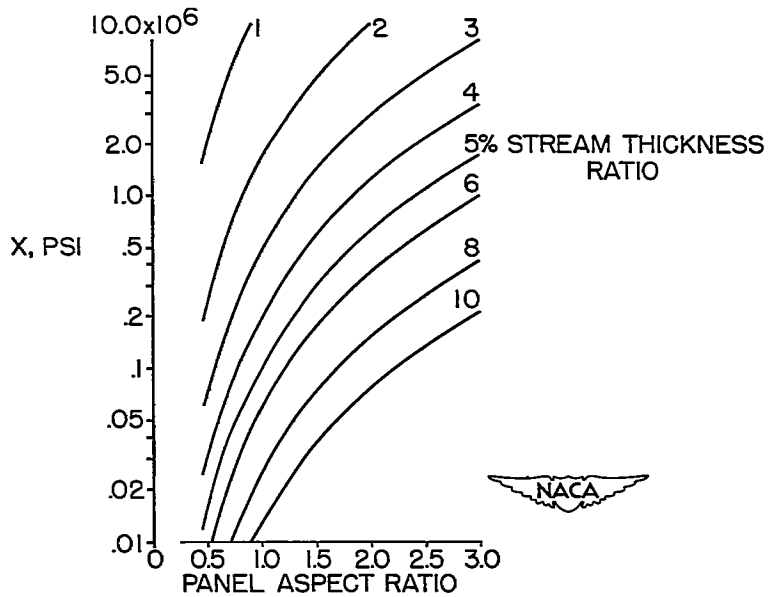


Figure 4.- The parameter X as a function of panel aspect ratio and thickness ratio.

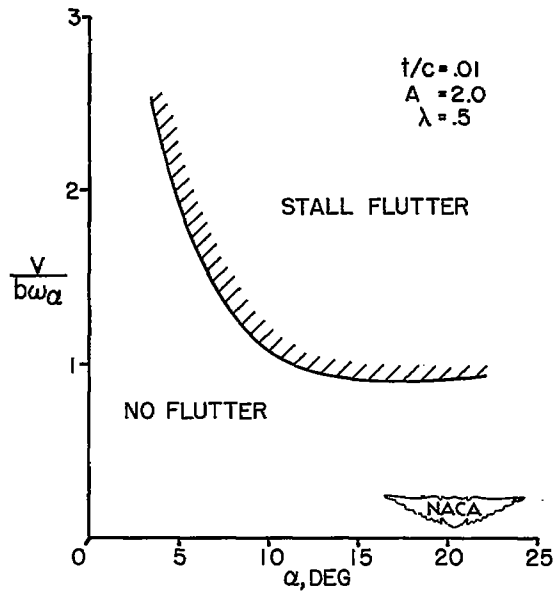


Figure 5.- Flutter behavior of a typical wing at angles of attack.

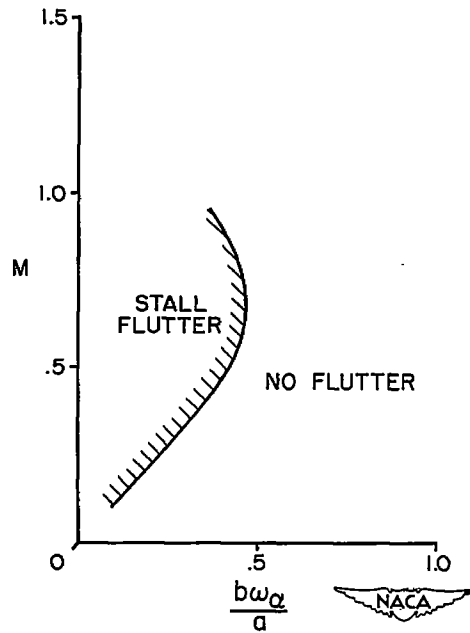


Figure 6.- Trend study of stall flutter.

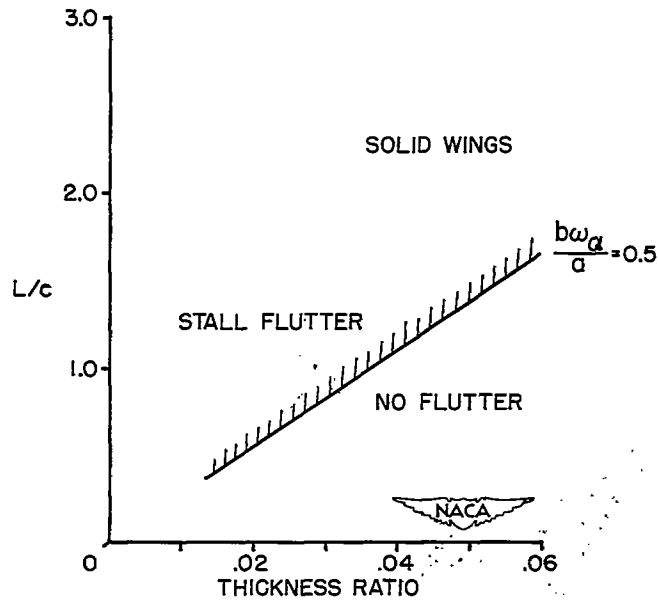


Figure 7.- Composite chart for stall flutter of solid unswept wings.

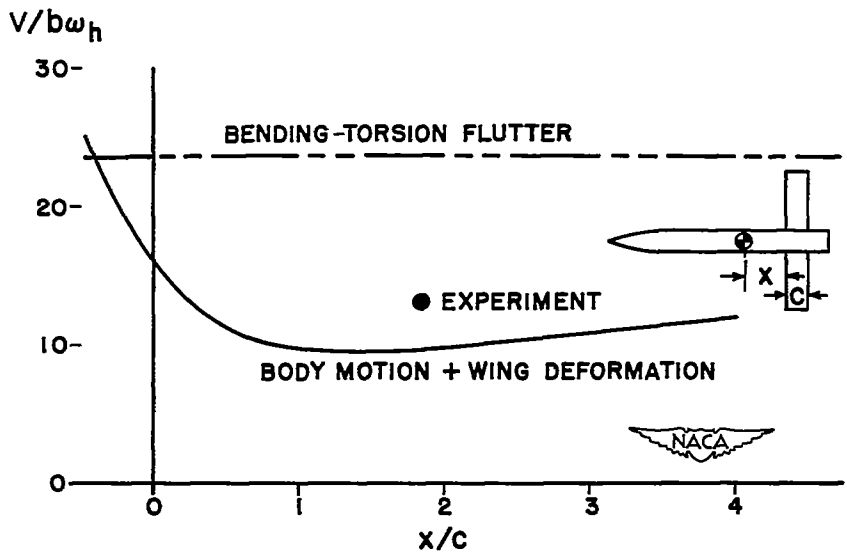


Figure 8.- Study of flutter involving body modes.